Geophysical Research Letters

RESEARCH LETTER
10.1029/2024GL110847

Observational Constraints on the Spatial Effect of Greenness and Canopy Cover on Urban Heat in a Major Midlatitude City

Jangho Lee[1] **and Max Berkelhammer**[1]

[1]Earth and Environmental Sciences, University of Illinois Chicago, Chicago, IL, USA

Key Points:

- Greenery, canopy cover, and proximity to water lower heat index, while impervious cover raises heat index, especially in the afternoon
- Interactions exist between greenery, canopy cover, and impervious cover, affecting their combined impact on heat index
- Selecting impactful areas and using integrated approaches are crucial for effective urban heat reduction

Supporting Information:

Supporting Information may be found in the online version of this article.

Correspondence to:

J. Lee,
jholee@uic.edu

Citation:

Lee, J., & Berkelhammer, M. (2024). Observational constraints on the spatial effect of greenness and Canopy Cover on Urban Heat in a major midlatitude city. *Geophysical Research Letters*, *51*, e2024GL110847. https://doi.org/10.1029/2024GL110847

Received 18 JUN 2024
Accepted 14 OCT 2024

Abstract Urban heat stress is a critical issue, particularly in cities where dense infrastructure and limited green space exacerbate temperature extremes. This study investigates the impact of greenery (EVI2), canopy cover (CC), impervious cover (IC), and water bodies on heat index in Chicago using high-resolution data from the Heat Watch campaign. We find that EVI2, CC and proximity to water body significantly reduce heat while IC increases heat, particularly in the afternoon when solar radiation is intense. Additionally, the effective radius that land cover impacts heat is smaller in the afternoon. The combined effect analysis indicates that enhancing total greenness, not just canopy cover, is the most effective strategy to reduce heat. This study underscores the importance of strategic vegetation management, highlighting the critical role of integrated approaches in reducing urban heat.

Plain Language Summary This study looks at how greenery, tree canopy cover, impervious surfaces (like concrete), and water bodies affect air temperature in Chicago. Using detailed air temperature data from the Heat Watch campaign, we found that vegetation and proximity to water significantly reduce temperatures, while impervious surfaces increase temperatures, especially in the afternoon when the sun is strongest. The influence of these factors on temperature is more localized in the afternoon. Our analysis shows that increasing overall greenery, not just tree canopy cover, is the most effective way to reduce heat. This study highlights the importance of strategic vegetation management and integrated approaches to effectively reduce urban heat.

1. Introduction

Urban areas worldwide are experiencing rapid growth, leading to increased concerns regarding the urban heat island (UHI) effect, where urban temperatures are significantly higher than those in surrounding rural areas (Kim & Brown, 2021; Rizwan et al., 2008; Tzavali et al., 2015). This phenomenon is primarily driven by the replacement of natural vegetation with impervious surfaces, which absorb and retain heat. Climate change exacerbates this issue by increasing the frequency and intensity of heatwaves in the urban settings (Chapman et al., 2017; Parker, 2010; Sachindra et al., 2016). With over 80% of the US population living in the urban areas, elevated temperatures can adversely affect human health (Bell et al., 2018; Ebi et al., 2021; Lee & Dessler, 2023; Vaidyanathan et al., 2019), increase energy consumption (Dirks et al., 2015; Lee & Dessler, 2022; Morakinyo et al., 2019), and reduce overall urban sustainability (Mauree et al., 2019; Santamouris et al., 2020). Therefore, understanding the factors that influence urban heat and developing effective mitigation strategies are critical for improving the livability of the cities.

Previous studies have used both modeling and observational approaches to explore the efficacy of various strategies to cool urban environments, including increasing urban greenery through parks, green roofs, and street trees (Balany et al., 2020; Li et al., 2014; Marando et al., 2022). Additionally, the use of urban water bodies (Ghosh & Das, 2018; Steeneveld et al., 2014), such as fountains, and the application of reflective and high-albedo materials (Santamouris & Yun, 2020; Yang et al., 2015) have been investigated. Greenness and canopy cover, in particular, is widely considered effective due to its ability to decrease temperatures and its additional positive effects on human health and well-being. Though these are offset by increases in pollen and reductions in air quality, in some cases (Lovasi et al., 2013; Roman et al., 2021).

Urban greenery plays a crucial role in mitigating urban heat through mechanisms such as increases in evapotranspiration and the reduction of heat absorption by impervious surfaces. Metrics for greenery, such as the

Normalized Difference Vegetation Index (NDVI) and the Enhanced Vegetation Index (EVI), have been widely used to quantify the coverage and health of vegetation in urban areas (Chun & Guldmann, 2018; Marando et al., 2019). Furthermore, factors such as canopy cover (Chen et al., 2020; Tamaskani Esfehankalateh et al., 2021; Ziter et al., 2019) and impervious surface cover (Morabito et al., 2021; Yuan & Bauer, 2007) have been investigated as significant contributors to urban heat.

Canopy cover, a subset of urban greenery, specifically refers to the layer of leaves, branches, and stems of trees that provide direct shading and reduce solar radiation reaching the surface. However, it can also increase downward solar radiation with a decrease in albedo. On the other hand, urban greenery encompasses all types of vegetation, including grass, shrubs, and ground cover, which contribute to cooling through mechanisms like evapotranspiration and heat absorption reduction. Impervious surface cover tends to increase temperatures due to its high heat absorption and retention capabilities. However, there are uncertainties, particularly regarding the interactions between green and impervious spaces and how these effects vary with time of day. Diurnal variation is important, as the underlying mechanisms of daytime and nighttime heat variation differ (Logan et al., 2020; Shiflett et al., 2017), as do their impacts on human health (Davis et al., 2020; Martinez-Nicolas et al., 2014). Therefore, understanding the effects and interactions of vegetation indices, canopy cover, and impervious cover at different times of the day is essential for designing effective urban heat mitigation strategies (Erell & Zhou, 2022; Hu & Li, 2020; Huang et al., 2008).

Quantifying the impact of these variables on urban heat requires high-resolution data, which is often difficult to obtain. Land surface temperature (LST) measurements from satellites such as MODIS (Crosson et al., 2012; Mukherjee et al., 2017), Landsat (Cilek & Cilek, 2021; Yang et al., 2020), or ECOSTRESS (Hulley et al., 2019; Shi et al., 2022) have been extensively utilized for urban temperature analysis. However, these measurements are limited because they do not directly measure air temperature, which is the property that has a more direct impact on human comfort and health. Additionally, LST measurements do not account for cooling through advection, making it challenging to estimate the spatial scale and aggregated effects of cooling associated with different land covers. Lastly, satellite measurements have limitations in measuring surface humidity, which is another important factor to consider as a heat metric because it significantly impacts human health (Heo et al., 2019; Lu & Romps, 2023; Wehner et al., 2017). This is more important as humidity is understudied in most cities, whereas air temperature has been variable of interest in cities with denser measurement networks, such as Chicago (Li & Sharma, 2024b).

With these limitations on measurement techniques, vehicle measurement campaigns are commonly used to provide spatially extensive data in the absence of dense meteorological networks that are difficult to maintain in cities (Alonzo et al., 2021; Ziter et al., 2019). In this study, we leverage data from the Heat Watch campaign conducted in Chicago. This campaign provides high-resolution temperature and humidity data, which, when combined with satellite and land cover products, allows us to effectively quantify the role of greenery and land cover in the urban microclimate. This integrated approach helps us better understand the spatial and temporal dynamics of urban heat, providing valuable insights for urban heat mitigation strategies.

This study aims to address three critical questions for effectively utilizing greening to mitigate urban heat: the individual effect of greenness at different times of the day, the most effective buffer size for cooling, and the interactions between EVI2, canopy cover, and impervious cover. Understanding diurnal variations is crucial, as the impact of vegetation differs between morning and afternoon due to changes in solar radiation and atmospheric conditions. Additionally, determining the optimal buffer sizes is important, as different elements of urban landscapes, such as parks, tree-lined streets, and large water bodies, have varying spatial influences on temperature. Lastly, understanding how EVI2, canopy cover, and impervious cover interact is vital for developing targeted interventions, as these interactions can inform more nuanced and effective urban planning decisions.

2. Data

2.1. Heat Watch Data

Air temperature and humidity data for this study were obtained from the Heat Watch campaign in Chicago (CAPA/NIHHIS, 2023), part of the NOAA Urban Heat Island Mapping Campaign initiated in 2017. To measure air temperature and humidity, 100 volunteers navigated the city of Chicago with homogeneous measurement sensors mounted in their vehicles on 28 July 2023. The daily average temperature measured at O'Hare Airport in

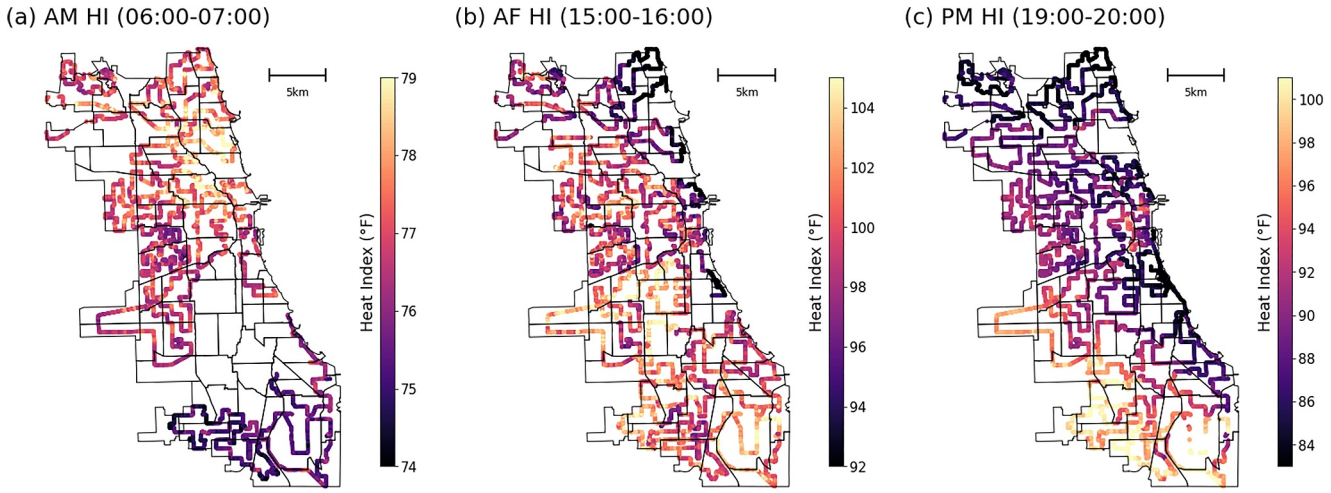

Figure 1. Heat index (HI) variations and measurement routes across Chicago at different times of the day. (a) AM HI (06:00–07:00), (b) AF HI (15:00–16:00), and (c) PM HI (19:00–20:00). The color gradients represent HI ranges.

Chicago during the 2023 summer months (June, July, and August) is 23.1°C, while the temperature on July 28 was 28.9°C. This indicates that the chosen day was a hotter than an average day in the Chicago summer but was not classified as a heat wave event. Data collection occurred during three distinct time windows on this day: early morning between 06:00 and 07:00 (AM), afternoon from 15:00 to 16:00 (AF), and evening from 19:00 to 20:00 (PM). A total of 139,443 air temperature (T) and relative humidity (RH) measurements were recorded from this campaign. Sunrise was at 5:40 a.m. and the sunset was at 8:13 p.m. local time at that day. Thus, AM and PM dataset are representative of time right before the sunrise and right before the sunset.

From the measured T and RH, we calculate heat index (HI), a metric that quantifies the perceived temperature by combining the effects of both temperature and humidity on human comfort (Rothfusz, 1990). The graphic of the measuring route and HI are shown in Figure 1. According to NOAA, generally a heat index above 80, 90, 105, and 125°F indicates caution, extreme caution, danger, and extreme danger, respectively. Formula that are used to calculate the heat index is shown in Supporting Information S1 Section S1. A description of T and specific humidity (SH), which is calculated from T and RH, can also be found in Supporting Information S1 Section S1.

2.2. Urban Land Cover Data

For the metric of greenery, we utilize satellite measurements from the PlanetScope constellation, operated by Planet Labs Inc. This constellation comprises over 180 CubeSats in sun-synchronous orbits, capturing multi-spectral imagery with a spatial resolution ranging from 3.7 to 4.1 m, depending on altitude. The PlanetScope instrument measures eight spectral bands: Coastal Blue (central wavelength: 443 nm), Blue (490 nm), Green 1 (531 nm), Green (565 nm), Yellow (610 nm), Red (665 nm), Red Edge (705 nm), and Near-Infrared (NIR, 865 nm). From these bands, we calculate the Enhanced Vegetation Index 2 (EVI2) as shown in Equation 1.

$$\mathrm{EVI2} = 2.5 \times \frac{(\mathrm{NIR} - \mathrm{RED})}{\mathrm{NIR} + (2.4 \times \mathrm{RED}) + 1} \quad (1)$$

EVI2 is selected for its superior representation of densely vegetated areas compared to other indices like the Normalized Difference Vegetation Index (NDVI). It offers advantages due to its heightened sensitivity to variations in canopy structure, including leaf area index, canopy type, and architecture—factors crucial for understanding the cooling effects of urban vegetation. In this study, we also evaluated other vegetation indices such as NDVI and the original EVI. However, we find that these alternatives do not significantly alter the overall findings. We use PlanetScope data from July 21 to 4 August 2023, a 2 week period that aligns with the Heat Watch campaign. Using median values for the entire summer of that year did not make a significant change in the conclusion of this study.

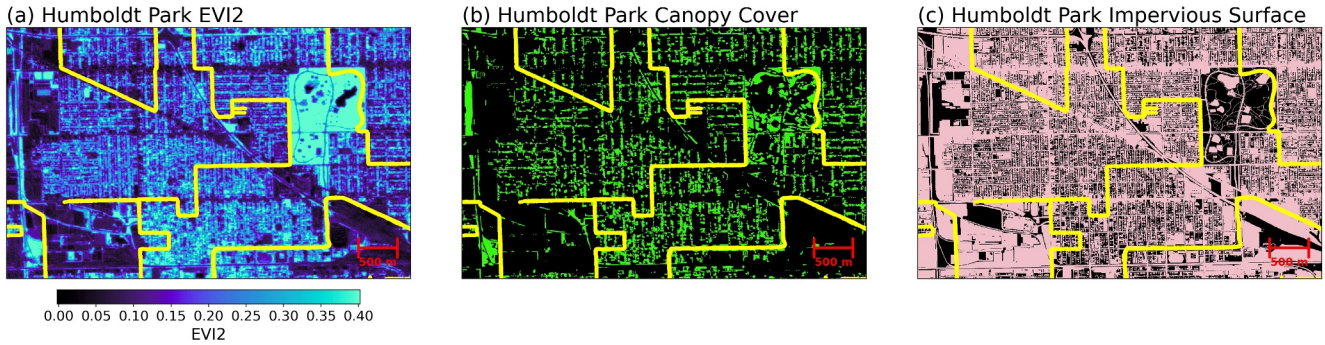

Figure 2. Spatial representation of environmental variables in Humboldt Park. (a) Enhanced Vegetation Index 2 (EVI2), indicating greenery, (b) Canopy Cover, showing the extent of tree cover (binary values), and (c) Impervious Cover, illustrating the extent of non-permeable surfaces (binary values). The yellow line represents the temperature measurement route.

One-meter resolution canopy cover and impervious land cover data were obtained from the NOAA Coastal Change Analysis Program (C-CAP) for the year 2021. This dataset includes three binary layers: canopy cover, impervious land cover, and water body. It is important to note the distinction between EVI2 and canopy cover. While both can serve as metrics of vegetation, EVI2 measures the greenness and density of vegetation, whereas canopy cover specifically represents the proportion of land area covered by the canopy of trees and other vegetation. Thus, a prairie or field might have a high greenness score, but low canopy cover and unhealthy trees might have high canopy cover but low greenness. Furthermore, we include impervious surface in our analysis because it significantly affects urban heat dynamics by heat retention and increasing surface temperatures.

We have three data sets: EVI2 (3 m resolution), canopy cover (1 m resolution), and impervious cover (1 m resolution), for the entire Chicago region. Subset of this data are shown in Figure 2 for the example in the Humboldt Park community area in Chicago. For each of the 139,443 measurements of Heat Watch data, we calculate the average EVI2 value, fraction of canopy cover (CC), and fraction of impervious cover (IC) within a given buffer around each measurement point. The radiuses of these buffers are: 10, 25, 50, 75, 100, 125, 150, 200, 250, 300, 350, 400, 450, and 500 m (14 cases in total). This allows us to examine the extent of each land cover's effects on local heat index, similar to previous studies (Alonzo et al., 2021; Ziter et al., 2019).

Lastly, we consider distance to water body (DW). We account only for significant water bodies larger than 1,000 m^2 to minimize the effect of small water bodies that might not be significant (e.g., small fountains). For each measurement point, we calculate the distance to the closest significant water body and add this as a predictor variable. Significant water bodies are very close to Lake Michigan on the eastern side of Chicago, so DW can be approximated to the distance to Lake Michigan in this study.

3. Method of Analysis

In this study, we use the Generalized Additive Model (GAM) as the main statistical method. GAM is particularly effective for analyzing the curvature and non-linear effects of each predictor variable since it allows for the inclusion of smooth functions to model relationships that are not strictly linear. This flexibility enables us to capture complex patterns in the data, enhancing the accuracy of our analysis regarding urban heat dynamics. We set up our model as follows:

$$HI_{t,b} \approx GAM_{t,b}(s(DW) + s(EVI2_b) + s(CC_b) + s(IC_b) + te(EVI2_b, CC_b, IC_b)) \quad (2)$$

where $HI_{t,b}$ represents the heat index at a specific time of day t (AM, AF, and PM) and within a buffer radius b (14 values ranging from 10 to 500 m). Thus, there are 52 (3×14) GAMs built for each time of the day and buffer sizes. Each s () term represents a spline term, a smooth function constituting four three-order polynomial curves, capturing the individual effects of each predictor variable: DW, EVI2, CC, and IC. The te () term represents the tensor product, which is an interaction term between EVI2, CC and IC, accounting for their combined effect. This model setup is similar to previous studies that utilize multiple predictors for urban air temperature and heat analysis (Alonzo et al., 2021; Johnson et al., 2020; Trlica et al., 2017; Zhang et al., 2024; Ziter et al., 2019). For

each term, we calculate the partial dependence to quantify the effect of each variable by fixing all other terms while changing the term of interest. For AM, AF, and PM, there are 38,518, 47,541, and 49,400 measurement samples, respectively, used to build the GAMs.

4. Results

4.1. Individual Effects

First, we examine the individual effect of EVI2 on HI, as shown in Figure 3. We also conducted a similar analysis on T and SH individually, rather than on the HI, to determine the contribution of each factor to HI. Overall, we found that HI is predominantly influenced by T rather than SH. Detailed analyses of T and SH are provided in Supporting Information S1 Section S2. Furthermore, analysis regarding multicollinearity between the predictor variables are discussed in Supporting Information S1 Section S3.

Analyzing the effect of EVI2 on micro-scale HI (Figures 3a–3c), the effect is most significant in the AF, followed by PM and AM. This is because higher solar radiation during the AF period enhances the cooling effect of greenery due to increased evapotranspiration rates. The most significant buffer size of EVI2 contributing to HI is 10 m in the AM and AF, and 25 m in the PM. This indicates that smaller vegetation patches have a more localized cooling effect during periods of intense solar radiation, while in the evening, larger areas of vegetation are more effective at reducing heat index due to the accumulated cooling effect over a broader area. Additionally, non-linearity is observed, especially in the AF, as the buffer size increases beyond 300 m. This indicates the absence of a clear large-scale effect of EVI2, particularly for lower EVI2 values (under 0.2), in the AF when solar radiation is high and the direct cooling effect of EVI2 is more relevant.

CC exhibits a similar pattern to EVI2 as in previous studies (Alonzo et al., 2021; Ziter et al., 2019), as depicted in Figures 3d–3f. However, a notable difference is observed in the most effective buffer size. While EVI2 had a more localized effect with 10 and 25 m buffer, CC shows the most effective buffer size at 100 and 125 m throughout the day. This suggests that canopy cover has a broader spatial influence compared to the greenness index. This could be related to the fact that the trees in Chicago are quite large—so the canopy cover increases surface frication and boundary layer dynamics leading to larger spatial scale of impact (Li & Sharma, 2024a). This highlights the importance of widespread tree cover in urban areas for effective cooling. Furthermore, non-linearity is significant feature of the cooling effect from CC. The results show that increasing CC from about 0.25 to 0.5 is most effective for cooling, as the slope of the curve is steepest. This suggests an optimal range for canopy density. Increasing CC in regions with too little or too much canopy cover does not yield significant cooling benefits.

Next, we examine the impact of IC. The effect of IC is most prominent in the PM, followed by AF and AM. After sunset, the main driver of nighttime heat index variation is the heat retained by these impervious surfaces, resulting in a larger effective radius of influence (400 m), compared to AF, when the driver is direct solar radiation (10 m). Furthermore, the effect of IC is generally linear in AM and PM but exhibits a non-linear relationship in AF for larger buffers. This non-linearity is likely due to the localized nature of the heating effect during periods of high solar radiation. In the AF, impervious surfaces quickly absorb and re-radiate heat, leading to steep heat index increases over smaller areas. As the buffer size increases, the effect of impervious surfaces starts to level off, showing diminishing effect on HI for larger areas.

Finally, we consider the effect of DW on HI, as shown in Figure 3j. The cooling effect of proximity to water is evident, with the most significant impact observed in the AF, followed by PM, and a negligible effect in AM. In the afternoon, high solar radiation increases the temperature contrast between heat-absorbing land surfaces and heat-moderating water bodies, leading to significant cooling effects in areas near water. In the evening, as land surfaces begin to cool, the temperature of water bodies does not cool as much due to their high heat capacity. This reduces the cooling effect of DW on HI, as the thermal gradient between land and water decreases. In the morning, the effect of proximity to water on temperature is minimal. By this time, the thermal gradient between water bodies and land have evened out, resulting in a reduced cooling influence from the water. Humidity declines as DW increases, but the contribution of humidity to the HI is not substantial enough to offset the effect of T.

The choice of heat index can potentially affect the compensatory impact of humidity on urban heat stress (Chakraborty et al., 2022). To explore this, we tested various heat stress indices, including the wet-bulb temperature, which serves as a measure of how effectively humans can cool down through sweating (Sherwood & Huber, 2010). Our findings did not show a significant change in conclusions regardless of the index used. The

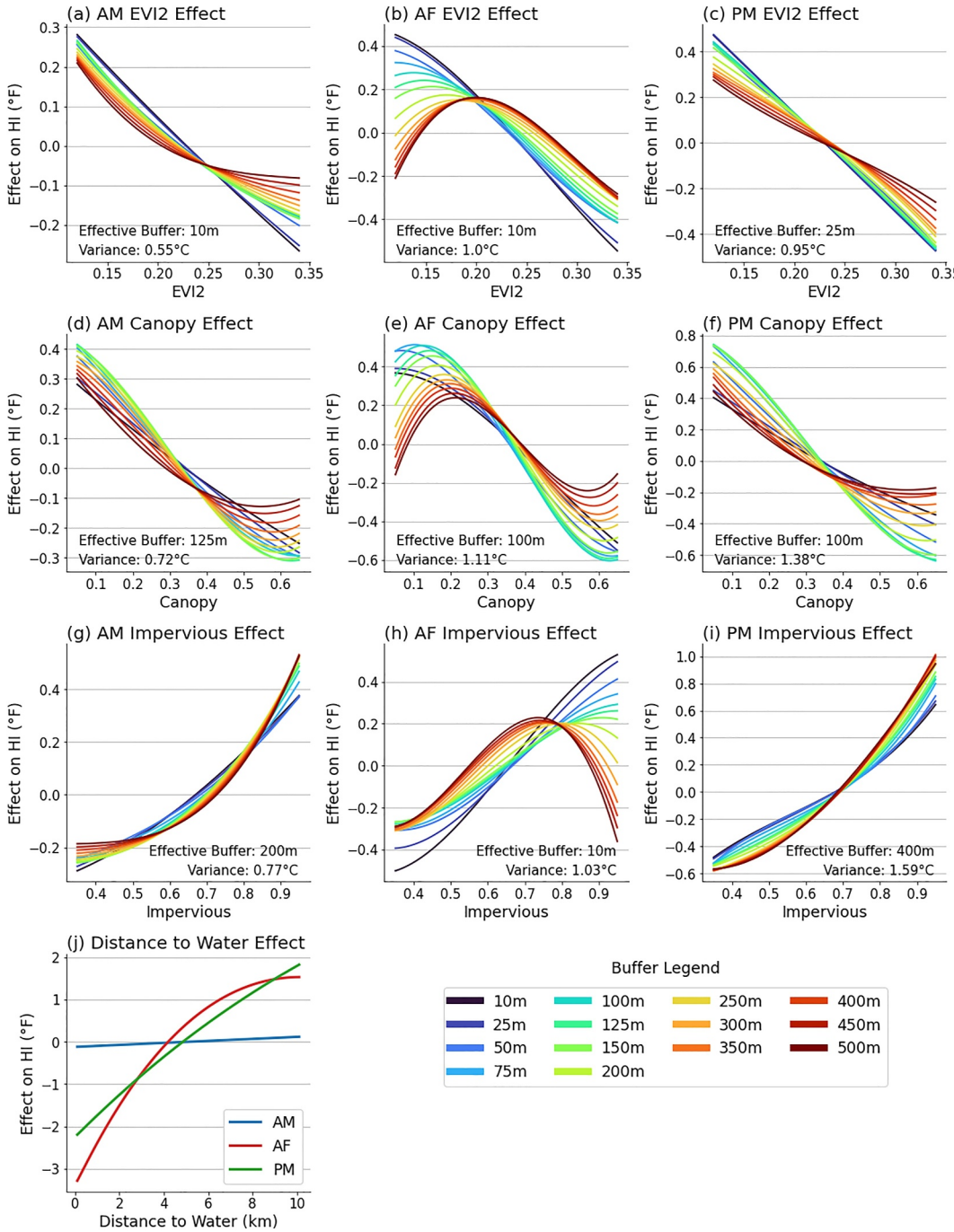

Figure 3. The relative effects of EVI2, Canopy Cover, Impervious Cover, and Distance to Water on het index (HI) across different times of the day. (a–c) EVI2 effects in AM, AF, and PM. The color-coded lines represent different buffer sizes ranging from 10 to 500 m (d–f) same as (a–c), but for Canopy Cover. (g–i) Same as (a–c) bur for Impervious Cover. (j) Distance to Water effects in AM (blue), AF (red), and PM (green).

results using the wet-bulb temperature, instead of the heat index (HI) employed in this study, are provided in Supporting Information S1 Section S2.

4.2. Combined Effect

Although EVI2, CC, and IC all have individual effects, it is important to examine the interaction between these datasets. For instance, will increasing CC in regions with high EVI2 have the same effect as in regions with low

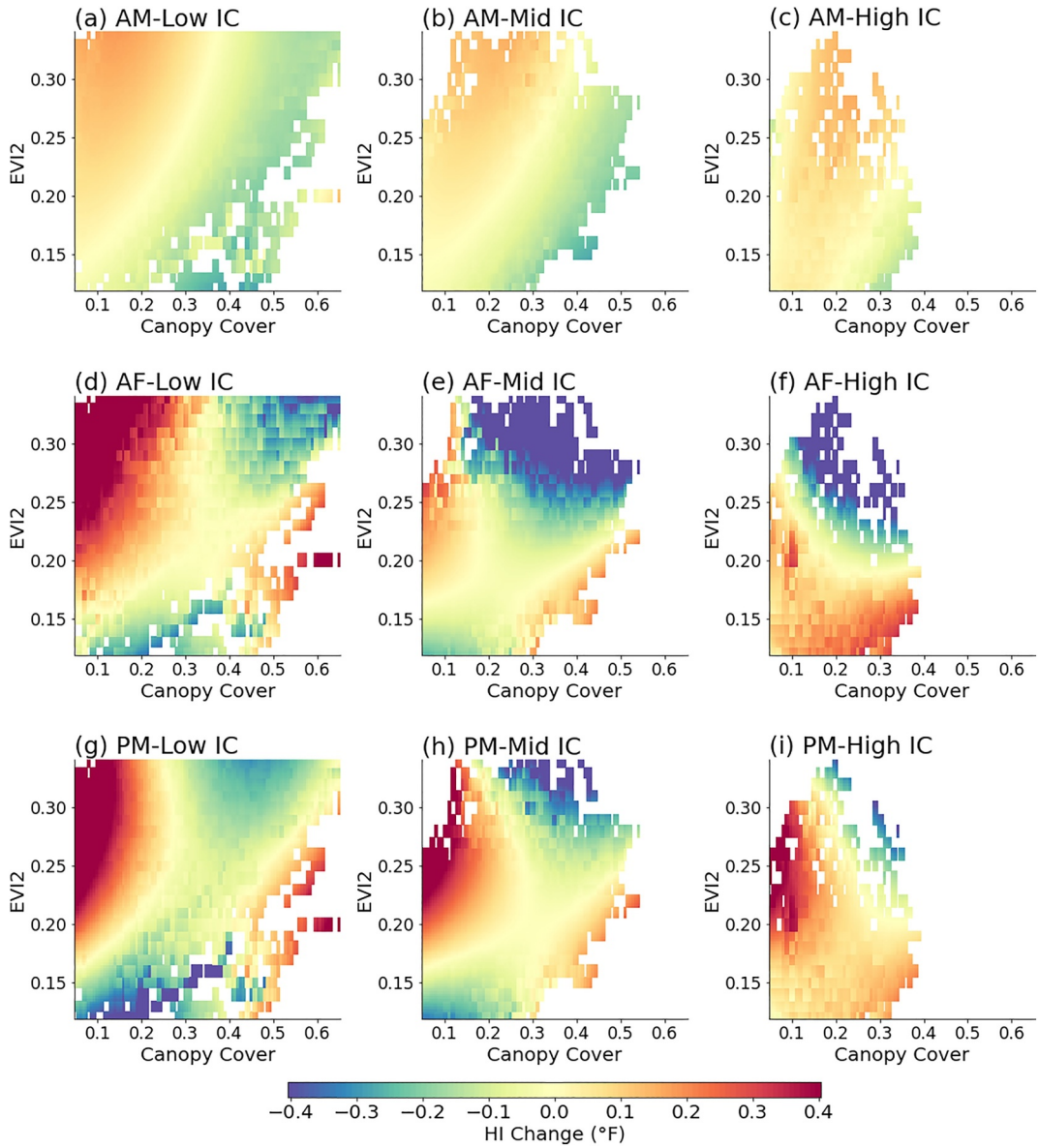

Figure 4. Interaction effects of Enhanced Vegetation Index 2 (EVI2) and Canopy Cover (CC) on heat index change (HI Change) across different times of the day and levels of Impervious Cover (IC). (a–c) Morning (AM) effects at low, mid, and high IC levels respectively. (d–f) Same as (a–c), bur for afternoon (AF) effects. (g–i) Same as (a–c) bur for evening (PM) effects. The color gradients represent heat index changes, with lower heat index shown in blue and higher heat index shown in red.

EVI2? Will these effects be consistent across different levels of IC? To address these questions, we analyze the interaction term in Equation 2. In Figure 4, we visualize the interaction term between EVI, CC and IC at a buffer size of 100 m ($b = 100$). To effectively illustrate this, we categorize IC into three bins: low (25th percentile), middle (50th percentile), and high (75th percentile). Each bin spans 10 percentile points, averaging dependencies within these ranges (e.g., 20th–30th percentile). For each low, middle, and high IC bin, we visualize the interaction term between EVI2 and CC. The heatmaps in Figures 4a–4i display the combined effect of EVI2 and CC on HI change across different times of the day (AM, AF, PM) and IC levels. Note that the combination of variables outside the observation range is masked out in the figure. Furthermore, interaction terms across different buffer sizes were tested, but the overall conclusions remain consistent (Supporting Information S1 Section S4).

Overall, the combined effect of EVI2, CC, and IC is most pronounced in the AF, followed by PM and AM. In the AM (Figures 4a–4c), the combined effect is less than 0.1°F and shows a similar magnitude and pattern across all IC levels. We find that at all EVI2 levels, increasing CC further decreases HI with its combined effect. Conversely, at low CC levels, increasing EVI2 (such as lawns) appears to increase HI. However, this should not be interpreted as EVI2 having a heating effect. As shown in Figure 3, increasing EVI2 individually has a cooling effect with a higher magnitude. Therefore, the observed increase in HI with low CC levels and increased EVI2 should be understood as a less effective cooling effect rather than an actual heating effect.

In the AF with low IC (Figures 4d–4f), the pattern is similar to AM, but with a higher magnitude. However, in the medium and high IC (Figures 4e and 4f), increasing EVI2 shows a decreasing effect on HI across all CC levels, unlike in the low IC (Figure 4d). This indicates that increasing greenness is particularly effective for cooling in afternoon, for medium to higher levels of impervious surfaces. Furthermore, significant cooling effect by CC in all levels of EVI2 indicate that shading can be the most significant mechanism during AF, under direct solar radiation.

In the PM (Figures 4g–4i), it is notable that EVI2 has a suppressing effect on HI cooling at low CC levels, and CC also has a suppressing effect on HI cooling at low EVI2 levels. This suggests that, for effective cooling during the evening, both high EVI2 and high CC are necessary. The combined presence of EVI2 and CC maximizes the cooling effect by enhancing evapotranspiration and increasing the roughness of the surface (i.e., more mixing), which reduces heat retention in the urban environment.

5. Implications and Conclusions

This study explores the individual and combined effects of Enhanced Vegetation Index 2 (EVI2), Canopy Cover (CC), Impervious Cover (IC), and Distance to Water (DW) on urban heat index (HI) at different times of the day and different buffer sizes. From these findings, we can derive the way land surface cover influences effective urban heat mitigation strategies in Chicago for different periods of the day.

5.1. Cooling Morning Heat (AM HI)

For the cooling of AM HI, EVI2 is effective on a very local scale (10 m buffer), and it is most beneficial to increase EVI2 in areas where EVI2 is low, rather than in high EVI2 regions. CC and IC are important in larger buffers (125 and 200 m). The effect of CC is nearly linear in the AM, indicating that increasing CC will have a consistent cooling effect around that region. However, the effect of IC is non-linear, making it particularly crucial to mitigate increases of IC in already high IC regions. To maximize the cooling effect through the combined effects, it is important to increase both EVI2 and CC simultaneously. We find that focusing on increasing EVI2 only in low CC regions can result in ineffective cooling in the morning. Therefore, a balanced approach of increasing the health and greenness of green spaces along with generating tree canopy is essential.

5.2. Cooling Afternoon Heat (AF HI)

In the AF, the effects of EVI2, CC, and IC all show non-linearity. The effective buffer is smaller at 10 m for EVI2 and IC, and 100 m for CC. To reduce HI in the AF, it is effective to increase EVI2 to above 0.2, as values below 0.2 do not significantly decrease HI. For CC, focusing on regions with CC around 0.2 and increasing them to 0.4 is most effective, as this range shows the greatest cooling effect. This insight is particularly important for urban tree planting programs, as it helps determine the most effective locations for planting. Like many cities, Chicago has a tree planting program that is managed at neighborhood scales and these findings can be used to optimize these efforts. For IC, it is crucial to decrease IC in regions below 0.7, as areas with IC above 0.7 do not experience significant cooling even with reductions in IC. For the combined effect, it is important to increase both EVI2 and CC. However, it is especially critical to increase CC in mid and high IC regions. By enhancing both EVI2 and CC, but prioritizing CC in high IC areas, urban heat mitigation can be more effectively achieved during the hottest part of the day.

5.3. Cooling Evening Heat (PM HI)

In the PM, the pattern of the effects of EVI2, CC, and IC is similar with the AF, but the non-linearity decreases. Additionally, the effective buffer for IC increases, so that IC have more larger effect. Furthermore, IC has highest impact on PM HI, meaning that retained heat from impervious surfaces is the main driver of urban heat in the PM.

For the reduction of PM HI, increasing EVI2 and CC at all levels and decreasing IC at all levels is effective, as the non-linearity is much less pronounced than in the AF. For the combined effect, it remains important to increase both EVI2 and CC. However, it is more effective to increase CC alone than to increase EVI2 alone.

5.4. Conclusions

This study highlights the critical role of vegetation indices and land cover types in urban heat mitigation strategies. Consistent with previous studies, we find that the effect of land cover varies depending on the time of day due to different physical mechanisms such as direct shading, canopy mixing, and urban heat retention. Additionally, we observe that different buffer sizes of vegetation have varying degrees of effectiveness in reducing urban heat. Our analysis further demonstrates that strategic increases in EVI2 and CC, coupled with reductions in IC and DW, can effectively reduce urban heat index. The findings also emphasize the importance of considering the interactions between these variables to maximize cooling benefits. Specifically, increasing CC in conjunction with EVI2 proves to be more effective than increasing EVI2 alone. Incorporating large water bodies within urban environments can also provide substantial cooling benefits, particularly during the afternoon. Moreover, the strategic selection of locations and targeted approaches for implementing these measures are essential for maximizing their efficiency and effectiveness.

By implementing these strategies, cities can mitigate the urban heat island effect, improve thermal comfort, and promote sustainable urban living. Effective urban heat mitigation requires not only increasing greenery and reducing impervious surfaces but also carefully selecting the most impactful areas and employing integrated approaches to ensure the best outcomes. These selections should not only focus on heat reduction but also consider socio-economic factors, addressing environmental justice issues to ensure that all communities, particularly those historically underserved or disproportionately affected by heat, benefit equitably from urban cooling efforts (Lee et al., 2024; McDonald et al., 2024; Mitchell & Chakraborty, 2015). Moreover, the idea of co-design is crucial, where neighborhoods might prioritize specific target criteria (such as reducing energy consumption) over others (such as reducing heat risk from outdoor work). These approaches can be laid out, discussed, and prioritized through iterative design processes, and then implemented through community-based programs.

6. Limitations and Future Directions

This study is not without its limitations. First, it only focused on heat index in Chicago on 1 day in the summer, making it difficult to generalize the results to other cities or seasons. However, the features observed here are consistent with results from Madison, WI (Ziter et al., 2019) suggesting the results might be generalizable. Secondly, the CC and IC data used are 2 years apart from the heat data, as the C-CAP data are from 2021 while the Heat Watch campaign was conducted in 2023. Although changes in CC and IC over 2 years are likely minimal, this discrepancy introduces some uncertainty into the analysis. Thirdly, the measurements were conducted from vehicles, resulting in a bias since all data were collected on impervious surfaces (roads). It would be beneficial to have data measured by humans, allowing for a broader range of land covers, such as the middle of parks. Unfortunately, this was not the case in this study. Additionally, the measurements were conducted within a 1 hr window. However, time-dependent normalization or standardization of the measurements was not performed to account for heat index fluctuations within that hour. Lastly, this study only considered EVI2, CC, IC, and DW. Other meteorological variables, such as wind speed and direction, can also impact heat index and could be included in future analyses to provide a more comprehensive understanding of urban heat dynamics.

Conflict of Interest

The authors declare no conflicts of interest relevant to this study.

Data Availability Statement

Heat Watch temperature data is available online (CAPA/NIHHIS, 2023). PlanetScope data is available upon request to Planet Labs Inc by accessing: https://www.planet.com/contact-sales/. NOAA C-CAP data for canopy and impervious land cover data is available online (www.coast.noaa.gov/htdata/raster1/landcover/bulkdownload/hires/).

Acknowledgments
This material is based upon work supported by the U.S. Department of Energy, Office of Science, Office of Biological and Environmental Research's Urban Integrated Field Laboratories CROCUS project research activity, under Award Number DE-SC0023226.

References

Alonzo, M., Baker, M. E., Gao, Y., & Shandas, V. (2021). Spatial configuration and time of day impact the magnitude of urban tree canopy cooling. *Environmental Research Letters*, *16*(8), 084028. https://doi.org/10.1088/1748-9326/ac12f2

Balany, F., Ng, A. W., Muttil, N., Muthukumaran, S., & Wong, M. S. (2020). Green infrastructure as an urban heat island mitigation strategy—A review. *Water*, *12*(12), 3577. https://doi.org/10.3390/w12123577

Bell, J. E., Brown, C. L., Conlon, K., Herring, S., Kunkel, K. E., Lawrimore, J., et al. (2018). Changes in extreme events and the potential impacts on human health. *Journal of the Air and Waste Management Association*, *68*(4), 265–287. https://doi.org/10.1080/10962247.2017.1401017

CAPA/NIHHIS. (2023). Heat Watch Chicago [Dataset]. OSF. Retrieved from: https://osf.io/6d7p2/

Chakraborty, T., Venter, Z., Qian, Y., & Lee, X. (2022). Lower urban humidity moderates outdoor heat stress. *AGU Advances*, *3*(5), e2022AV000729. https://doi.org/10.1029/2022av000729

Chapman, S., Watson, J. E., Salazar, A., Thatcher, M., & McAlpine, C. A. (2017). The impact of urbanization and climate change on urban temperatures: A systematic review. *Landscape Ecology*, *32*(10), 1921–1935. https://doi.org/10.1007/s10980-017-0561-4

Chen, J., Jin, S., & Du, P. (2020). Roles of horizontal and vertical tree canopy structure in mitigating daytime and nighttime urban heat island effects. *International Journal of Applied Earth Observation and Geoinformation*, *89*, 102060. https://doi.org/10.1016/j.jag.2020.102060

Chun, B., & Guldmann, J.-M. (2018). Impact of greening on the urban heat island: Seasonal variations and mitigation strategies. *Computers, Environment and Urban Systems*, *71*, 165–176. https://doi.org/10.1016/j.compenvurbsys.2018.05.006

Cilek, M. U., & Cilek, A. (2021). Analyses of land surface temperature (LST) variability among local climate zones (LCZs) comparing Landsat-8 and ENVI-met model data. *Sustainable Cities and Society*, *69*, 102877. https://doi.org/10.1016/j.scs.2021.102877

Crosson, W. L., Al-Hamdan, M. Z., Hemmings, S. N., & Wade, G. M. (2012). A daily merged MODIS Aqua–Terra land surface temperature data set for the conterminous United States. *Remote Sensing of Environment*, *119*, 315–324. https://doi.org/10.1016/j.rse.2011.12.019

Davis, R. E., Hondula, D. M., & Sharif, H. (2020). Examining the diurnal temperature range enigma: Why is human health related to the daily change in temperature? *International Journal of Biometeorology*, *64*(3), 397–407. https://doi.org/10.1007/s00484-019-01825-8

Dirks, J. A., Gorrissen, W. J., Hathaway, J. H., Skorski, D. C., Scott, M. J., Pulsipher, T. C., et al. (2015). Impacts of climate change on energy consumption and peak demand in buildings: A detailed regional approach. *Energy*, *79*, 20–32. https://doi.org/10.1016/j.energy.2014.08.081

Ebi, K. L., Capon, A., Berry, P., Broderick, C., de Dear, R., Havenith, G., et al. (2021). Hot weather and heat extremes: Health risks. *The Lancet*, *398*(10301), 698–708. https://doi.org/10.1016/s0140-6736(21)01208-3

Erell, E., & Zhou, B. (2022). The effect of increasing surface cover vegetation on urban microclimate and energy demand for building heating and cooling. *Building and Environment*, *213*, 108867. https://doi.org/10.1016/j.buildenv.2022.108867

Ghosh, S., & Das, A. (2018). Modelling urban cooling island impact of green space and water bodies on surface urban heat island in a continuously developing urban area. *Modeling Earth Systems and Environment*, *4*(2), 501–515. https://doi.org/10.1007/s40808-018-0456-7

Heo, S., Bell, M. L., & Lee, J.-T. (2019). Comparison of health risks by heat wave definition: Applicability of wet-bulb globe temperature for heat wave criteria. *Environmental Research*, *168*, 158–170. https://doi.org/10.1016/j.envres.2018.09.032

Hu, L., & Li, Q. (2020). Greenspace, bluespace, and their interactive influence on urban thermal environments. *Environmental Research Letters*, *15*(3), 034041. https://doi.org/10.1088/1748-9326/ab6c30

Huang, L., Li, J., Zhao, D., & Zhu, J. (2008). A fieldwork study on the diurnal changes of urban microclimate in four types of ground cover and urban heat island of Nanjing, China. *Building and Environment*, *43*(1), 7–17. https://doi.org/10.1016/j.buildenv.2006.11.025

Hulley, G., Shivers, S., Wetherley, E., & Cudd, R. (2019). New ECOSTRESS and MODIS land surface temperature data reveal fine-scale heat vulnerability in cities: A case study for Los Angeles County, California. *Remote Sensing*, *11*(18), 2136. https://doi.org/10.3390/rs11182136

Johnson, S., Ross, Z., Kheirbek, I., & Ito, K. (2020). Characterization of intra-urban spatial variation in observed summer ambient temperature from the New York City Community Air Survey. *Urban Climate*, *31*, 100583. https://doi.org/10.1016/j.uclim.2020.100583

Kim, S. W., & Brown, R. D. (2021). Urban heat island (UHI) intensity and magnitude estimations: A systematic literature review. *Science of the Total Environment*, *779*, 146389. https://doi.org/10.1016/j.scitotenv.2021.146389

Lee, J., Berkelhammer, M., Wilson, M. D., Love, N., & Cintron, R. (2024). Urban land surface temperature downscaling in Chicago: addressing ethnic inequality and gentrification. *Remote Sensing*, *16*(9), 1639. https://doi.org/10.3390/rs16091639

Lee, J., & Dessler, A. E. (2022). The impact of neglecting climate change and variability on ercot's forecasts of electricity demand in Texas. *Weather, Climate, and Society*, *14*(2), 499–505. https://doi.org/10.1175/wcas-d-21-0140.1

Lee, J., & Dessler, A. E. (2023). Future temperature-related deaths in the US: The impact of climate change, demographics, and adaptation. *GeoHealth*, *7*(8), e2023GH000799. https://doi.org/10.1029/2023gh000799

Li, D., Bou-Zeid, E., & Oppenheimer, M. (2014). The effectiveness of cool and green roofs as urban heat island mitigation strategies. *Environmental Research Letters*, *9*(5), 055002. https://doi.org/10.1088/1748-9326/9/5/055002

Li, P., & Sharma, A. (2024a). Hitab-chicago: Height Map of trees and buildings for the city of Chicago. Retrieved from https://doi.org/10.5281/zenodo.10463648

Li, P., & Sharma, A. (2024b). Hyper-local temperature prediction using detailed urban climate informatics. *Journal of Advances in Modeling Earth Systems*, *16*(3), e2023MS003943. https://doi.org/10.1029/2023ms003943

Logan, T., Zaitchik, B., Guikema, S., & Nisbet, A. (2020). Night and day: The influence and relative importance of urban characteristics on remotely sensed land surface temperature. *Remote Sensing of Environment*, *247*, 111861. https://doi.org/10.1016/j.rse.2020.111861

Lovasi, G. S., O'Neil-Dunne, J. P., Lu, J. W., Sheehan, D., Perzanowski, M. S., MacFaden, S. W., et al. (2013). Urban tree canopy and asthma, wheeze, rhinitis, and allergic sensitization to tree pollen in a New York City birth cohort. *Environmental Health Perspectives*, *121*(4), 494–500. https://doi.org/10.1289/ehp.1205513

Lu, Y.-C., & Romps, D. M. (2023). Is a wet-bulb temperature of 35∘ C the correct threshold for human survivability? *Environmental Research Letters*, *18*(9), 094021. https://doi.org/10.1088/1748-9326/ace83c

Marando, F., Heris, M. P., Zulian, G., Udías, A., Mentaschi, L., Chrysoulakis, N., et al. (2022). Urban heat island mitigation by green infrastructure in European Functional Urban Areas. *Sustainable Cities and Society*, *77*, 103564. https://doi.org/10.1016/j.scs.2021.103564

Marando, F., Salvatori, E., Sebastiani, A., Fusaro, L., & Manes, F. (2019). Regulating ecosystem services and green infrastructure: Assessment of urban heat island effect mitigation in the municipality of Rome, Italy. *Ecological Modelling*, *392*, 92–102. https://doi.org/10.1016/j.ecolmodel.2018.11.011

Martinez-Nicolas, A., Madrid, J. A., & Rol, M. A. (2014). Day–night contrast as source of health for the human circadian system. *Chronobiology International*, *31*(3), 382–393. https://doi.org/10.3109/07420528.2013.861845

Mauree, D., Naboni, E., Coccolo, S., Perera, A. T. D., Nik, V. M., & Scartezzini, J.-L. (2019). A review of assessment methods for the urban environment and its energy sustainability to guarantee climate adaptation of future cities. *Renewable and Sustainable Energy Reviews*, *112*, 733–746. https://doi.org/10.1016/j.rser.2019.06.005

McDonald, R. I., Biswas, T., Chakraborty, T., Kroeger, T., Cook-Patton, S. C., & Fargione, J. E. (2024). Current inequality and future potential of US urban tree cover for reducing heat-related health impacts. *npj Urban Sustainability*, *4*(1), 18. https://doi.org/10.1038/s42949-024-00150-3

Mitchell, B. C., & Chakraborty, J. (2015). Landscapes of thermal inequity: Disproportionate exposure to urban heat in the three largest US cities. *Environmental Research Letters*, *10*(11), 115005. https://doi.org/10.1088/1748-9326/10/11/115005

Morabito, M., Crisci, A., Guerri, G., Messeri, A., Congedo, L., & Munafò, M. (2021). Surface urban heat islands in Italian metropolitan cities: Tree cover and impervious surface influences. *Science of the Total Environment*, *751*, 142334. https://doi.org/10.1016/j.scitotenv.2020.142334

Morakinyo, T. E., Ren, C., Shi, Y., Lau, K. K.-L., Tong, H.-W., Choy, C.-W., & Ng, E. (2019). Estimates of the impact of extreme heat events on cooling energy demand in Hong Kong. *Renewable Energy*, *142*, 73–84. https://doi.org/10.1016/j.renene.2019.04.077

Mukherjee, S., Joshi, P., & Garg, R. D. (2017). Analysis of urban built-up areas and surface urban heat island using downscaled MODIS derived land surface temperature data. *Geocarto International*, *32*(8), 900–918. https://doi.org/10.1080/10106049.2016.1222634

Parker, D. E. (2010). Urban heat island effects on estimates of observed climate change. *Wiley Interdisciplinary Reviews: Climate Change*, *1*(1), 123–133. https://doi.org/10.1002/wcc.21

Rizwan, A. M., Dennis, L. Y., & Chunho, L. (2008). A review on the generation, determination and mitigation of Urban Heat Island. *Journal of Environmental Sciences*, *20*(1), 120–128. https://doi.org/10.1016/s1001-0742(08)60019-4

Roman, L. A., Conway, T. M., Eisenman, T. S., Koeser, A. K., Ordóñez Barona, C., Locke, D. H., et al. (2021). Beyond 'trees are good': Disservices, management costs, and tradeoffs in urban forestry. *AMBIO*, *50*(3), 615–630. https://doi.org/10.1007/s13280-020-01396-8

Rothfusz, L. P. (1990). *The heat index equation (or, more than you ever wanted to know about heat index* (p. 640). National Oceanic and Atmospheric Administration, National Weather Service, Office of Meteorology, 9023.

Sachindra, D., Ng, A., Muthukumaran, S., & Perera, B. (2016). Impact of climate change on urban heat island effect and extreme temperatures: A case-study. *Quarterly Journal of the Royal Meteorological Society*, *142*(694), 172–186. https://doi.org/10.1002/qj.2642

Santamouris, M., Paolini, R., Haddad, S., Synnefa, A., Garshasbi, S., Hatvani-Kovacs, G., et al. (2020). Heat mitigation technologies can improve sustainability in cities. An holistic experimental and numerical impact assessment of urban overheating and related heat mitigation strategies on energy consumption, indoor comfort, vulnerability and heat-related mortality and morbidity in cities. *Energy and Buildings*, *217*, 110002. https://doi.org/10.1016/j.enbuild.2020.110002

Santamouris, M., & Yun, G. Y. (2020). Recent development and research priorities on cool and super cool materials to mitigate urban heat island. *Renewable Energy*, *161*, 792–807. https://doi.org/10.1016/j.renene.2020.07.109

Sherwood, S. C., & Huber, M. (2010). An adaptability limit to climate change due to heat stress. *Proceedings of the National Academy of Sciences*, *107*(21), 9552–9555. https://doi.org/10.1073/pnas.0913352107

Shi, Z., Yang, J., Wang, L.-e., Lv, F., Wang, G., Xiao, X., & Xia, J. (2022). Exploring seasonal diurnal surface temperature variation in cities based on ECOSTRESS data: A local climate zone perspective. *Frontiers in Public Health*, *10*, 1001344. https://doi.org/10.3389/fpubh.2022.1001344

Shiflett, S. A., Liang, L. L., Crum, S. M., Feyisa, G. L., Wang, J., & Jenerette, G. D. (2017). Variation in the urban vegetation, surface temperature, air temperature nexus. *Science of the Total Environment*, *579*, 495–505. https://doi.org/10.1016/j.scitotenv.2016.11.069

Steeneveld, G. J., Koopmans, S., Heusinkveld, B. G., & Theeuwes, N. E. (2014). Refreshing the role of open water surfaces on mitigating the maximum urban heat island effect. *Landscape and Urban Planning*, *121*, 92–96. https://doi.org/10.1016/j.landurbplan.2013.09.001

Tamaskani Esfehankalateh, A., Ngarambe, J., & Yun, G. Y. (2021). Influence of tree canopy coverage and leaf area density on urban heat island mitigation. *Sustainability*, *13*(13), 7496. https://doi.org/10.3390/su13137496

Trlica, A., Hutyra, L., Schaaf, C., Erb, A., & Wang, J. (2017). Albedo, land cover, and daytime surface temperature variation across an urbanized landscape. *Earth's Future*, *5*(11), 1084–1101. https://doi.org/10.1002/2017ef000569

Tzavali, A., Paravantis, J. P., Mihalakakou, G., Fotiadi, A., & Stigka, E. (2015). Urban heat island intensity: A literature review. *Fresenius Environmental Bulletin*, *24*(12b), 4537–4554.

Vaidyanathan, A., Saha, S., Vicedo-Cabrera, A. M., Gasparrini, A., Abdurehman, N., Jordan, R., et al. (2019). Assessment of extreme heat and hospitalizations to inform early warning systems. *Proceedings of the National Academy of Sciences*, *116*(12), 5420–5427. https://doi.org/10.1073/pnas.1806393116

Wehner, M., Castillo, F., & Stone, D. (2017). The impact of moisture and temperature on human health in heat waves. In *Oxford research encyclopedia of natural hazard science*.

Yang, J., Wang, Z.-H., & Kaloush, K. E. (2015). Environmental impacts of reflective materials: Is high albedo a 'silver bullet' for mitigating urban heat island? *Renewable and Sustainable Energy Reviews*, *47*, 830–843. https://doi.org/10.1016/j.rser.2015.03.092

Yang, Z., Witharana, C., Hurd, J., Wang, K., Hao, R., & Tong, S. (2020). Using Landsat 8 data to compare percent impervious surface area and normalized difference vegetation index as indicators of urban heat island effects in Connecticut, USA. *Environmental Earth Sciences*, *79*(18), 1–13. https://doi.org/10.1007/s12665-020-09159-0

Yuan, F., & Bauer, M. E. (2007). Comparison of impervious surface area and normalized difference vegetation index as indicators of surface urban heat island effects in Landsat imagery. *Remote Sensing of Environment*, *106*(3), 375–386. https://doi.org/10.1016/j.rse.2006.09.003

Zhang, X., Yang, F., Zhang, J., & Dai, Q. (2024). Using GAMs to explore the influence factors and their interactions on land surface temperature: A case study in Nanjing. *Land*, *13*(4), 465. https://doi.org/10.3390/land13040465

Ziter, C. D., Pedersen, E. J., Kucharik, C. J., & Turner, M. G. (2019). Scale-dependent interactions between tree canopy cover and impervious surfaces reduce daytime urban heat during summer. *Proceedings of the National Academy of Sciences*, *116*(15), 7575–7580. https://doi.org/10.1073/pnas.1817561116